U.S. Geological Survey Award Number G09AP00077

Final Technical Report

Near-Surface Geophysical Imaging of Paleochannels for the Determination of Slip Rate at the Green Valley Fault

Project Period: June 1st, 2009 - May 31st, 2010

Submitted September 9th, 2010

Mitchell S. Craig
Department of Earth and Environmental Sciences
California State University, East Bay
25800 Carlos Bee Blvd.
Hayward, CA 94542
Phone: 510-885-3425, Fax: 510-885-3486
mitchell.craig@csueastbay.edu

Key Words: near surface geophysics, seismic reflection, paleoseismology

U.S. Geological Survey Award Number G09AP00077

Final Technical Report

Near-Surface Geophysical Imaging of Paleochannels for the Determination of Slip Rate at the Green Valley Fault

Mitchell S. Craig
California State University, East Bay
mitchell.craig@csueastbay.edu

Abstract

Seismic reflection surveying was conducted at the Green Valley fault at Mason Road with the goal of identifying subsurface stream channels for use in measuring fault offset and slip rate. Three 180-m long, fault-parallel profiles were recorded north of Mason Road in August 2009 near the site of previous paleoseismologic investigations, including near-surface geophysical surveys. A 2007 seismic refraction survey south of Mason Road identified a trough-shaped, low-velocity body on the east side of the fault at depths of 5-12 m, which was interpreted as a stream channel truncated by the Green Valley fault. The present work was undertaken with the goal of finding the corresponding portion of the channel on the west side of the fault, presumably offset to the north due to motion on the fault during approximately the past 10-20 ka. Seismic reflection data were recorded in order to obtain higher-resolution and more extensive coverage. The new survey provided excellent resolution of near-surface stratigraphy at depths of 80-375 m, but did not provide sufficient resolution at shallower depths to permit correlation with data from the 2007 seismic refraction survey, which had a maximum depth penetration of only about 15 m. The new seismic reflection data appear to image lateral variations in fluvial stratigraphy at depths of approximately 100 m that could be used to measure fault offset in a future study.

Introduction

The Green Valley fault is located in a portion of the northeastern San Francisco Bay area (Frizzell and Brown, 1976) that is currently undeveloped but likely to undergo commercial and residential development in the coming decades. Based on trench studies of the fault at Mason Road and Lopes Ranch, Lienkaemper et al. (2008) documented at least four earthquakes large enough to cause surface rupture during the past 1000 years. In a study at Lopes Ranch, Baldwin et al. (2004), determined a geologic slip rate for the Green Valley fault of approximately 2-4 mm/yr based on approximately 30–60 m of displacement during the past 15 ka. These rates are consistent with the results of McFarland et al. (2007), who conducted theodolite surveys of the Green Valley fault and found the average creep rate at Mason Road since 2005 to be 2.8 mm/yr, and the average rate at Red Top Hill since 1984 to be 3.7 mm/yr. However, geodetic modeling of ongoing regional strain from GPS (Savage et al., 1999) suggests that the slip rate of the Green Valley fault may be as high as 10 mm/yr. The goal of the present study was to measure the slip rate of the fault during the past 10-20 ka by finding a buried stream channel that was deposited within this time range and subsequently offset by fault displacement.

Previous Work

A grid of nine fault-parallel seismic refraction profiles was recorded in 2007 with the goal of imaging paleochannels crossing the fault (Craig et al., 2008). The profiles were 92 m long and spaced 5 m apart, providing a 92 x 40 m footprint centered on the fault, with its long dimension oriented N-S, parallel to the fault. The line locations are indicated in yellow in Figure 1. Data were recorded using a 24-channel spread with 4 m receiver spacing, 24 m shot spacing, and 9 shot locations per profile. A tomographic velocity model was determined for each profile. All five profiles on the east side of the fault appeared to image a paleochannel, but the profiles on the west side did not. The abrupt truncation of the channel at the fault location suggested that it had been offset due to faulting, with the matching portion of the channel on the west side of the fault presumably displaced to the north. The base of the channel coincided with an abrupt increase in seismic velocity. Refraction profiles provided velocity information to 10-15 m depth. Velocities varied from 600 m/s near the surface to 1700 m/s at depth.

Sediment samples from a 7 m deep pit and auger hole south of Mason Road were dated using radiocarbon and OSL methods. Dates range from Holocene to late Pleistocene age. The pit was excavated in Summer 2005 to a depth of 7 m (Lienkaemper et al., 2007), and sediment samples were collected from sandy horizons and dated using the optically-stimulated luminescence (OSL) method. The deepest and oldest sample was from a depth of 5.6 m and was dated at 14.3 ± 0.43 ka. An auger hole located 135 m to the south, at CPT 13, encountered a coarse-grained layer at 11 m depth that was radiocarbon dated at 11-12 ka (J. Lienkaemper, personal communication). Cone-penetration testing (CPT) was conducted at the Mason Road site in 2004 by T. Noce of the USGS and in 2007 by Gregg Drilling. CPT holes were generally 10-15 m deep, with the deepest 25 m.

Reprocessing of 2007 Seismic Refraction Survey

Data from the 2007 seismic refraction survey were reprocessed in order to verify the previous results and interpretation, namely the presence of a truncated stream channel at 5-12 m depth on the east side of the fault. During reprocessing, special care was taken to ensure that all lines were processed consistently, including filters, picking first arrivals, parameters for traveltime inversion, and color scales for velocity displays. Geometrics Seisimager software was used to pick first arrivals and perform traveltime inversions to obtain velocity profiles (Figures 2 and 3).

New Seismic Reflection Survey: Acquisition and Processing

Seismic reflection data were acquired during August 2009. Lines were surveyed and staked out prior to mobilization of the seismic equipment and crew. Seismic data were recorded over the course of three days by a crew of three people. The survey consisted of three 180-m long profiles with 15 m line spacing (Figure 1). All three profiles were located on the north side of Mason

Road and on the west side of the fault. Recording parameters are listed in Table 1. Data quality was generally good to excellent, apart from some extended periods of severe noise from strong afternoon winds and an automatic pump from a nearby water well. The seismic survey was conducted in a privately-owned field that was normally under cultivation, but that was briefly available for data acquisition after the harvest of one crop and before plowing for the next. The recording surface was essentially flat, with gradually varying topography and less than 0.5 m of relief along the 180 m length of the profiles. The ground was dry, hard silty clay with no vegetation. The weather was sunny and hot.

Seismic reflection data were processed in the Windows environment using Parallel Geoscience Corporation (PGC) Seismic Processing Workshop (SPW) software, using standard methods (e.g., Sheriff and Geldart, 1995; Yilmaz et al., 2001), with some modifications to enhance resolution in the near-surface zone. Prestack gathers were filtered to eliminate low-frequency source-generated noise and high-frequency random noise, and edited to remove noisy traces (Figure 4). First breaks were eliminated at offsets greater than 6 m using a stovepipe mute (Figure 5). Near offset traces, at offsets of 3-6 m, were unmuted and served as the sole source of approximately the first 30 ms of data. Interactive semblance velocity analysis was performed using supergathers (Figure 6), and the velocity field for each of the three lines reviewed for any sharp lateral discontinuities in velocity and repicked as needed to provide a smooth field. Figure 7 shows the velocity field from line MA09-02 after the second pass of velocity analysis. Stacking velocities typically increased from about 1600 to 2200 m/s over the 100-300 ms range (Figure 8) and were well constrained by good data quality within this time range. The final stacked sections are shown in Figures 9-11. The data were processed only to 500 ms since the target of this study was the near-surface zone. A window of data from 0-300 ms was extracted from each of the three lines and the three windows were combined in Figure 12. The profiles in Figure 12 are labeled with both travel time and approximate depths that were calculated based on stacking velocities from line MA09-02. Common reflectors were correlated using colored horizons.

Results and Conclusions

The reprocessed velocity profiles from the 2007 seismic refraction survey (Figures 2 and 3) verified the general results and conclusions of the original processing, namely the presence of a truncated channel on the east side of the fault. All four lines on the east side of the fault (Figure 3) show a broad channel defined by the 1.7 km/s velocity contour at 10-12 m depth, while the lines on the west side (Figure 2) do not. The matching portion of the channel on the west side of the fault has presumably been displaced to the north due to right-lateral motion on the Green Valley fault. The velocity contours for all profiles on the east side of the fault appear to be displaced downward relative to those on the west side, indicating a component of vertical offset along the fault and a thicker layer of low velocity sediments on the east side of the fault.

The original processing of the data showed a narrower channel on the east side of the fault than what is indicated by the reprocessed data. The broader channel shown by the reprocessed data would be difficult to uniquely identify on the other side of the fault without additional, longer seismic lines on both sides of the fault.

The new seismic reflection survey clearly imaged stratigraphy over the time range 100-300 ms, corresponding to a depth range of about 80-375 m, but did not provide sufficient resolution at shallower depths to permit correlation with data from the 2007 seismic refraction survey. Arrivals prior to 50 ms tend to be dominated by energy from direct and refracted waves rather than reflections, and cannot be reliably used to interpret the near-surface stratigraphy.

The new data indicate sedimentary units that are relatively horizontal and planar, with some gentle undulations (Figures 9-11). Several of the reflectors exhibit lateral changes in character that likely correspond to lateral variations in bed thickness, including some pinchouts and bifurcations. These types of features are common in fluvial and alluvial fan environments, and could also indicate lithologic or facies changes. Lines MA09-02 and MA09-03 contain several reflectors with lateral changes in reflector character that may be associated the margins of fluvial channels, e.g., in the interval between horizons 3 and 5 in Figures 12b and 12c. The fact that similar lateral transitions occur in nearly the same location in all three lines gives us confidence that they are not artifacts due to transient noise during recording, but rather linear stratigraphic features that persist across several fault-parallel lines, and that could potentially be used as piercing points for measuring fault displacement.

Recommendations for further work

In order to measure fault offset at this location, two additional seismic profiles are needed, one on each side of the fault, using at least a 60-channel seismographic system with shot and geophone spacings of 3 meters or less. The profiles should be 600 m long, extending 200 m north of Mason Road and 400 m south of it. The longer profiles would provide the level of coverage needed to positively identify and match offset stratigraphic features on opposite sides of the fault. A Betsy Seisgun or equivalent source should be used to provide higher bandwidth and better resolution of shallow strata. Data acquisition should be suspended during periods of high noise caused by strong afternoon winds. New data should be processed using both refraction and reflection methods. With proper survey design and adequate quality control during data acquisition, these two methods can be used together to provide continuous coverage through the near-surface zone. The recommended work would be contingent upon the availability the field on the southern side of the road, which is scheduled for development in the near future.

The primary objective of this work was to search for paleochannels in the uppermost portion of the data, and this guided the data processing. As may be surmised from the stacked sections shown in Figures 9-11, clear reflections continue well beyond 500 ms where the data were

truncated. The data could be reprocessed utilizing the full original record length of 2.0 s to provide additional information on deeper stratigraphy well into the 500-1000 m depth range.

Education and student involvement

Four students from California State University, East Bay (CSUEB), including two undergraduates and two graduate students, participated in this project. Two students helped in the field with data acquisition, and three were involved with data processing. Data from this project were used for classroom instruction in two courses at Cal State East Bay: GEOL 4010 (Applied Geophysics) and GEOL 6200 (Advanced Topics - Exploration Seismology).

Acknowledgements

This work was supported by the U.S. Geological Survey, Award No. G09AP0007. Jim Lienkaemper (USGS) was instrumental in developing the study and provided ongoing encouragement and support. Uyanga Ganbaatar (CSUEB), Jonathan Arakaki (CSUEB), and Johnathan Brown (USGS) helped record the seismic surveys. Rufus Catchings and Mark Goldman (USGS) provided equipment used for data acquisition. Karen and Mike Waller, and Anthony Russo allowed access to their property for seismic surveying.

References

Baldwin, J. N.; Koehler, R. D.; Thompson, S. C., 2004, Preliminary Late Pleistocene Slip Rate of the Green Valley Fault at Lopes Ranch Creek, Cordelia, California, *Eos Trans. AGU*, 85(47), Fall Meet. Suppl., Abstract S31A-1027.

Craig, M. S., Kimball, M. A., Fay, R., and Lienkaemper, J. J., 2008, Near-Surface Geophysical Investigations of the Hayward and Green Valley Faults Using Seismic and Ground-Penetrating Radar Methods, *Seismological Research Letters*, 79(2), p. 316.

Craig, M., Lienkaemper, J., Crook, N., Dieter, B., Narvaez, R., and Nase, S., 2007, Near-surface geophysical surveying of the Green Valley fault, Fairfield CA, *Eos Trans. AGU*, *88*(52), Fall Meet. Suppl., Abstract NS24A-05.

Frizzell, V.A., Jr., and R.D. Brown, Jr., 1976, Map showing recently active breaks along the Green Valley fault, Napa and Solano Counties, California: United States Geological Survey, Miscellaneous Field Studies Map 743, 1:24000.

Lienkaemper, J. J., Sickler, R. R., Brown, J., Baldwin, J. N., Turner, R., Jr., and Guilderson, T. P., 2008, The Green Valley Fault: Geologic Record of Four Large Earthquakes in the Past Millennium (abstract), Third Conference on Earthquake Hazards in the Eastern San Francisco Bay Area.

McFarland, F. S., Lienkaemper, J. J., Caskey, S. J., and Grove, K., 2007, Data from Theodolite Measurements of Creep Rates on San Francisco Bay Region Faults, California: 1979-2007, USGS Open-File Report 2007-1367.

Savage, J. C., Svarc, J. L., Prescott, W. H., 1999, Geodetic estimates of fault slip rates in the San Francisco Bay area Journal of Geophysical Research. 104 (B3), pp. 4995-5002.

Sheriff, R. E. and Geldart, L. P., 1995, *Exploration Seismology, Second Edition*, Cambridge University Press, 592 pp.

Yilmaz, O., Doherty, S. M., & Yilmaz, O. (2001). *Seismic data analysis: Processing, inversion, and interpretation of seismic data*. Investigations in geophysics, no. 10. Tulsa, OK: Society of Exploration Geophysicists.

Recording parameters:

Shot spacing	3 m
Receiver spacing	3 m
CMP spacing	1.5 m
Source type	sledgehammer
Hammer blows per shot	3
Geophone frequency	40 Hz
Number of channels	60
Spread length	180 m
Minimum offset	0 m
Maximum offset	180 m
Sample interval	0.5 ms
Record length	2.0 s

Processing Sequence:

Convert from SEG-Y to SPW format.
Geometry assignment
Trace sort
Truncate data at t = 600 ms
Bulk shift -100 ms.
Band-pass filter: 40-150 Hz
Kill noisy traces
Spherical divergence correction, 4 dB/sec
Mute first arrivals
Sort to CMP gathers
Bin supergathers (5 CMPS per gather)
Semblance velocity analysis (15 m spacing)
Normal moveout (NMO) correction
Brute stack
Velocity field display
Semblance velocity analysis (2nd pass)
Final stack
Bandpass filter 40-150 Hz
f-x deconvolution

Table 1. Recording parameters and processing sequence for 2009 seismic reflection survey.

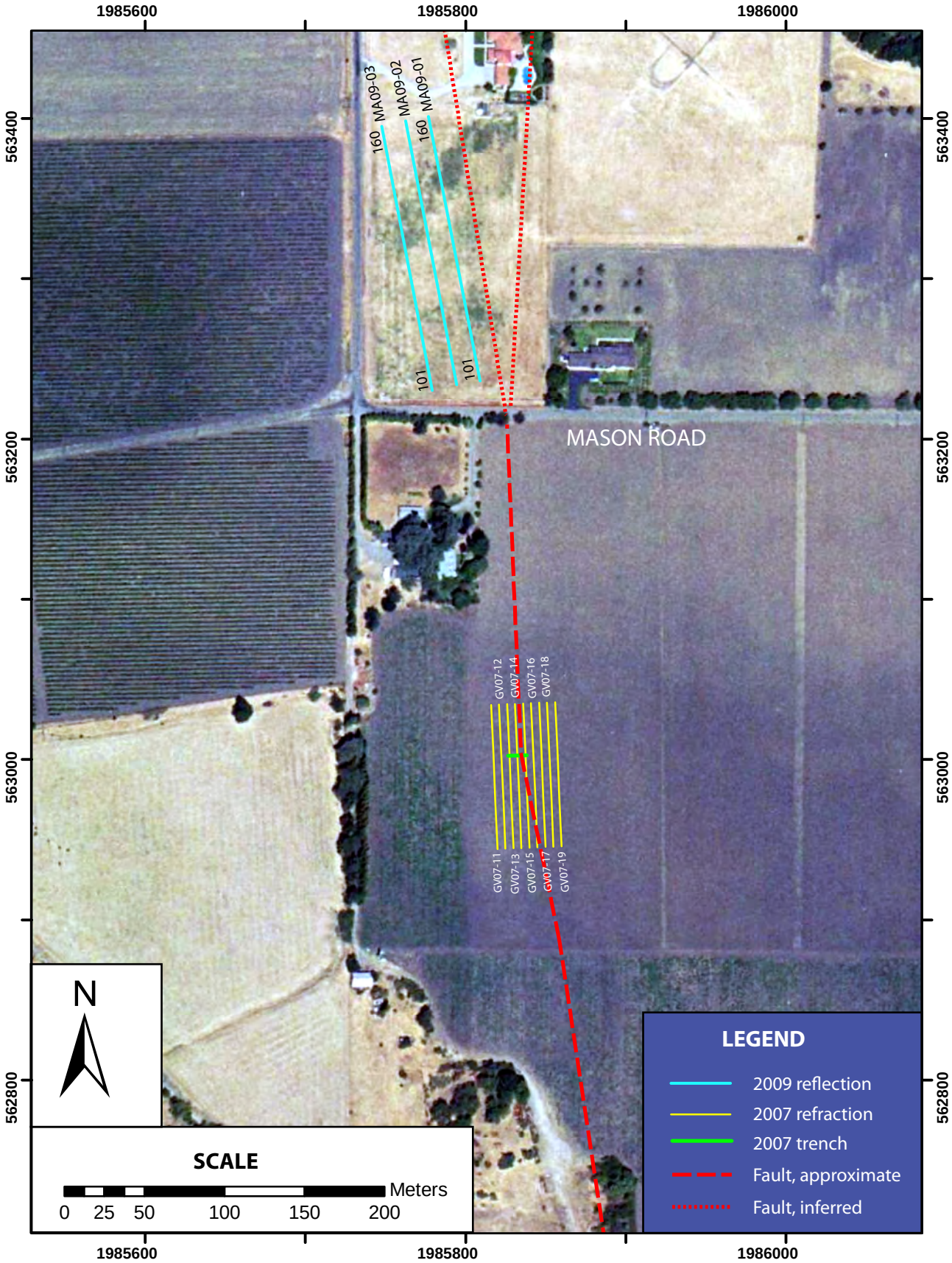

Figure 1. Basemap showing locations of 2009 seismic reflection lines (blue), 2007 seismic refraction lines (yellow), 2007 trench (green), and Green Valley fault (red). Fault trace and trench location courtesy J. Lienkaemper. Coordinates are NAD 1983 State Plane Coordinates in units of meters.

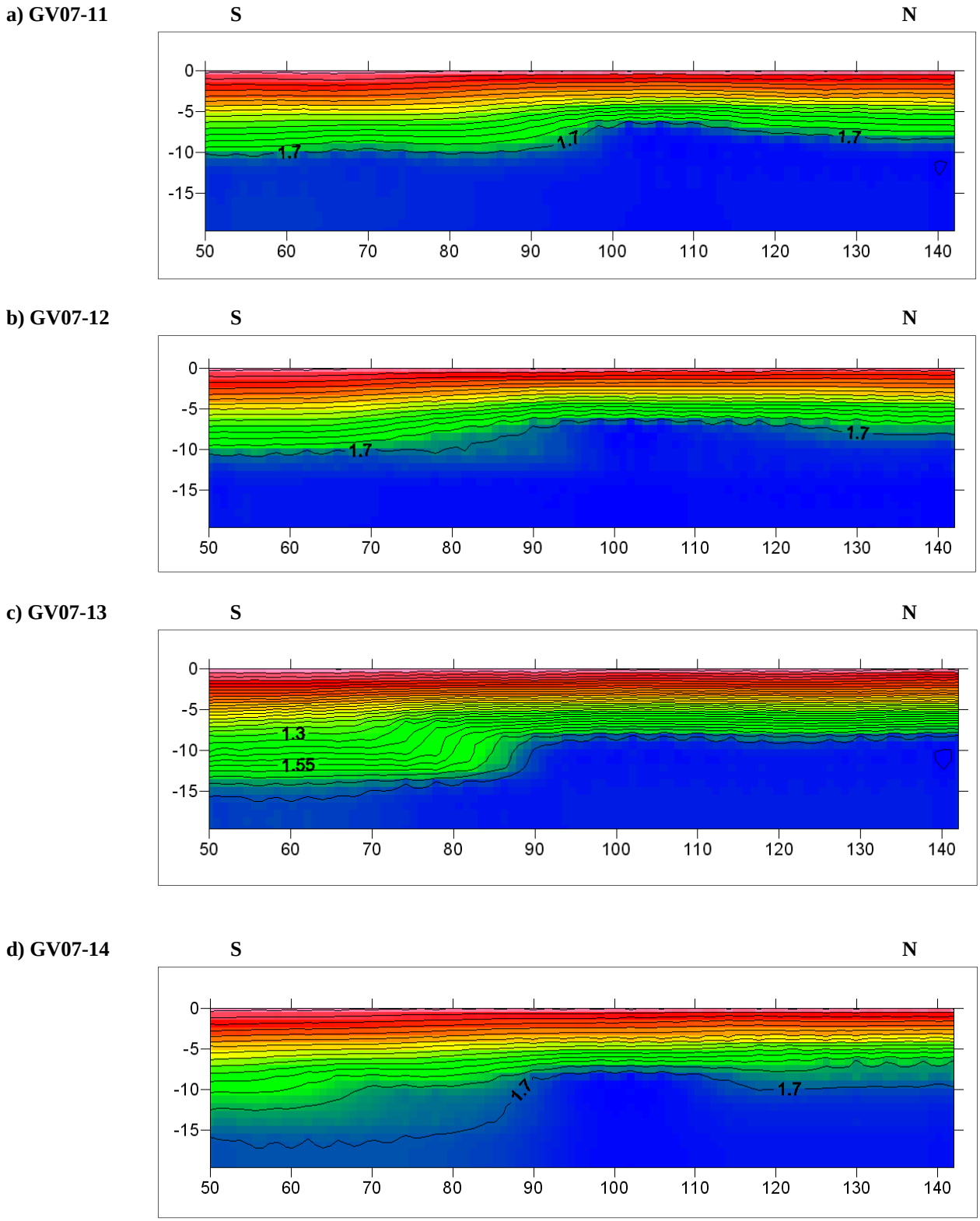

Figure 2. Seismic refraction profiles from 2007 survey on the west side of the Green Valley fault. Vertical scale is depth and horizontal scale is distance, both in units of meters. Contours are velocities in units of km/s, contour interval is 0.1 km/s. a) GV07-11, b) GV07-12, c) GV07-13, d) GV07-14. See Figure 1 for location map.

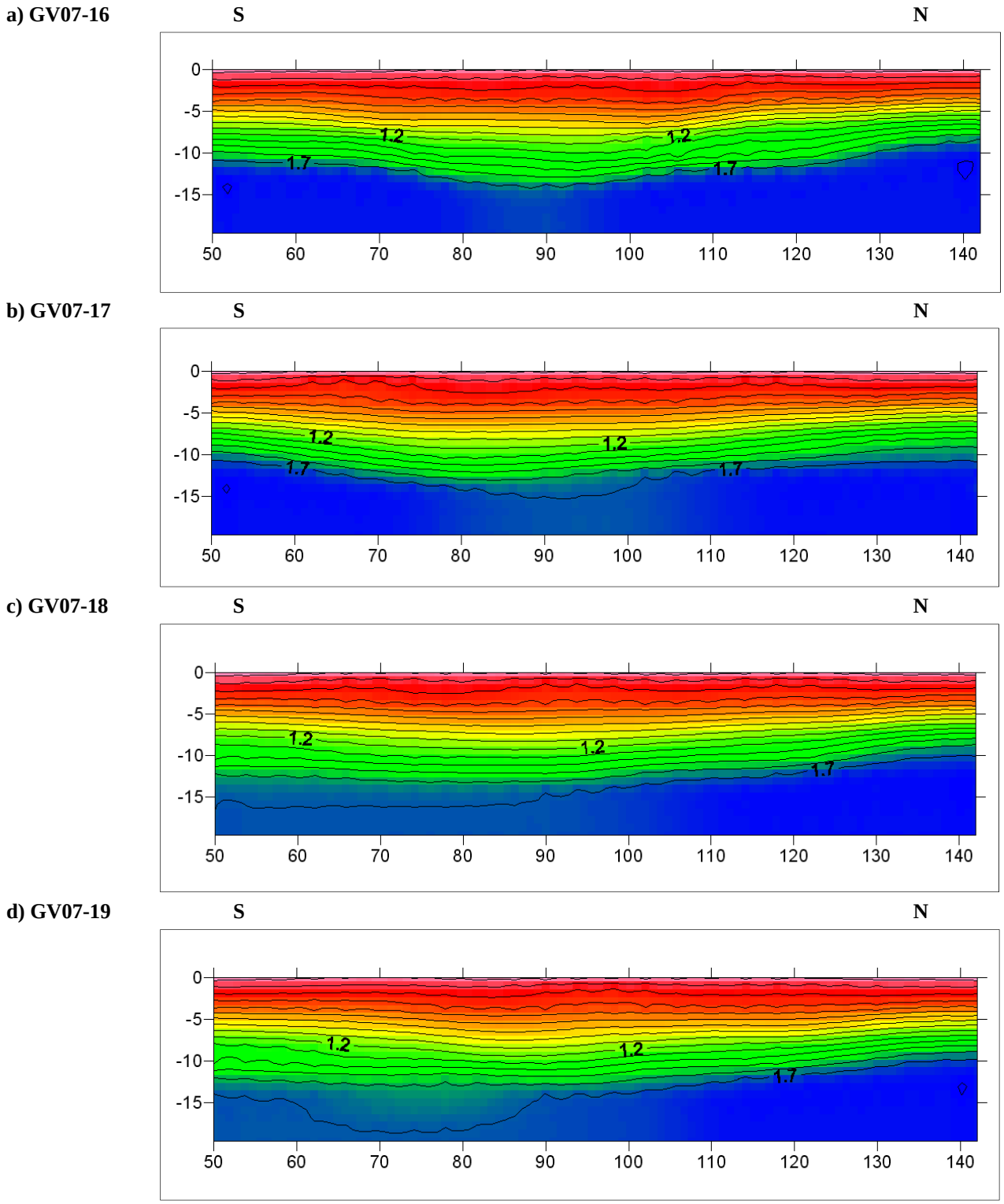

Figure 3. Seismic refraction profiles from 2007 survey on the east side of the Green Valley fault. Vertical scale is depth and horizontal scale is distance, both in units of meters. Contours are velocities in units of km/s, contour interval is 0.1 km/s. a) GV07-16, b) GV07-17, c) GV07-18, d) GV07-19. Note the similarity of the four profiles in this figure, and that the velocity contours in these profiles are displaced downward relative to those on the other side of the fault (Figure 2).

a)

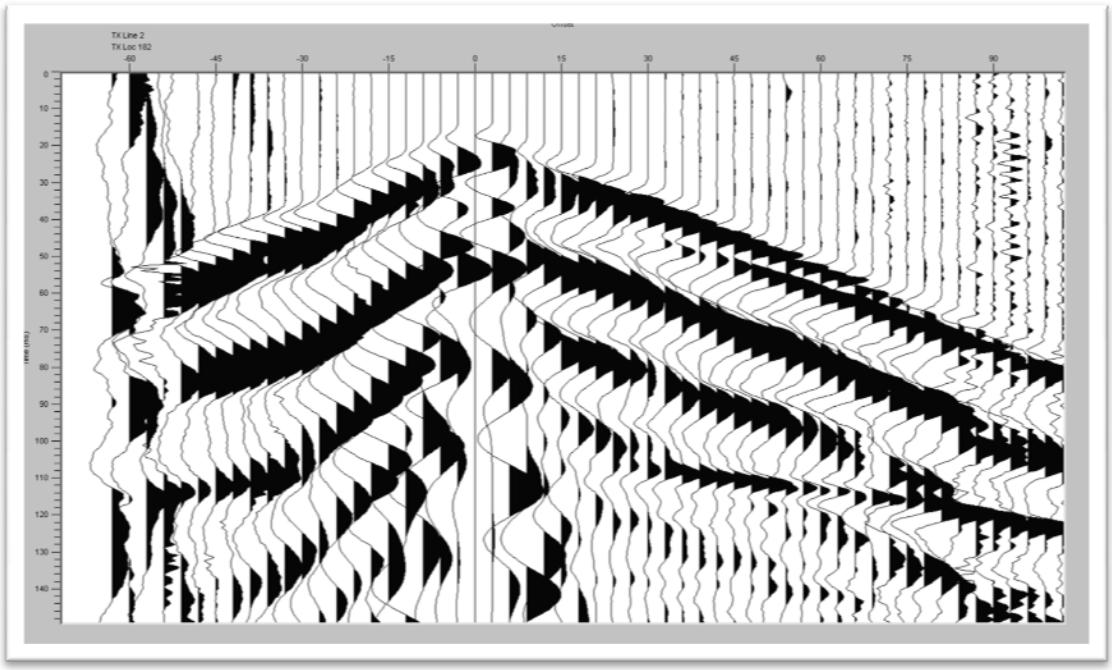

b)

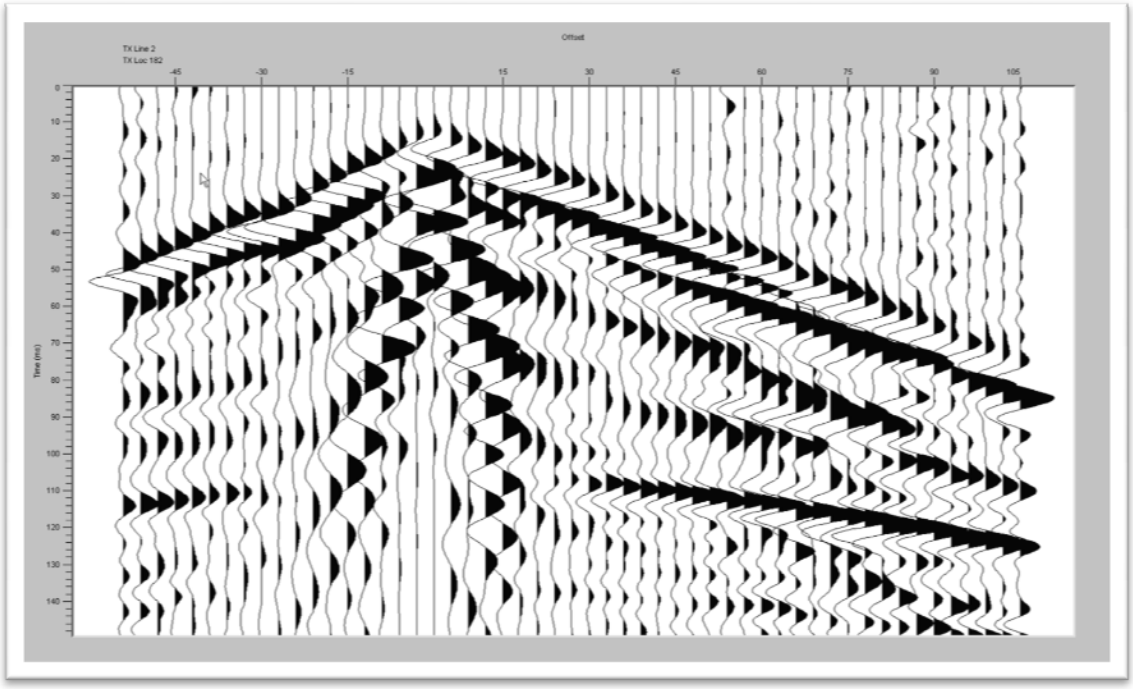

Figure 4. Filtering. a) Shot gather before filtering. The first few traces on the left-hand side of the gather are dominated by low-frequency noise, and some of the traces on right-hand side of the record contain high-frequency noise. b) The same shot gather after band-pass filter and removal of noisy traces.

a)

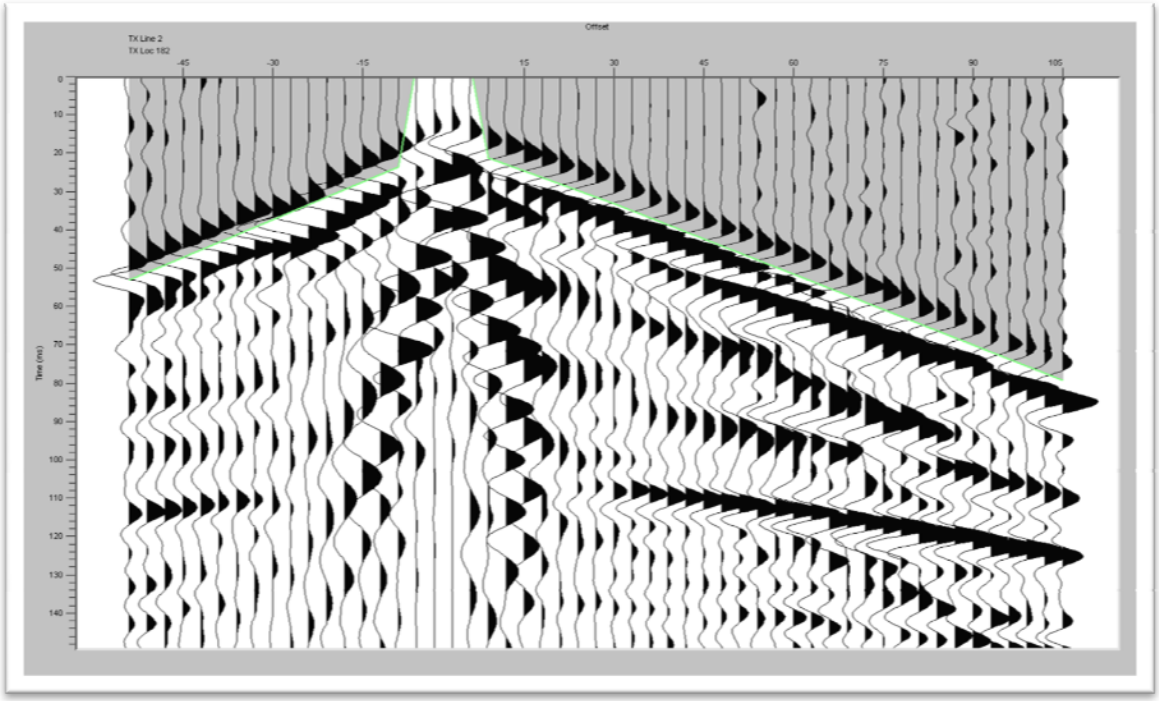

b)

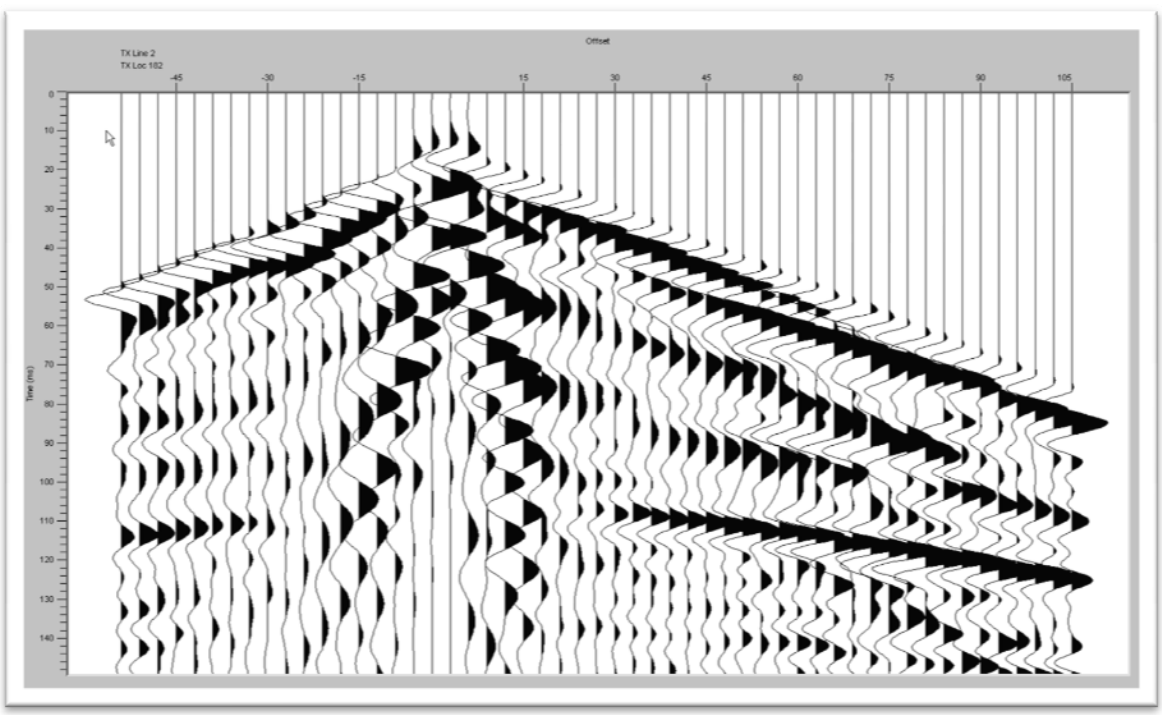

Figure 5. Muting. a) Shot gather with early mute superimposed. The portion of data shaded in gray will be muted. b) Shot gather after muting.

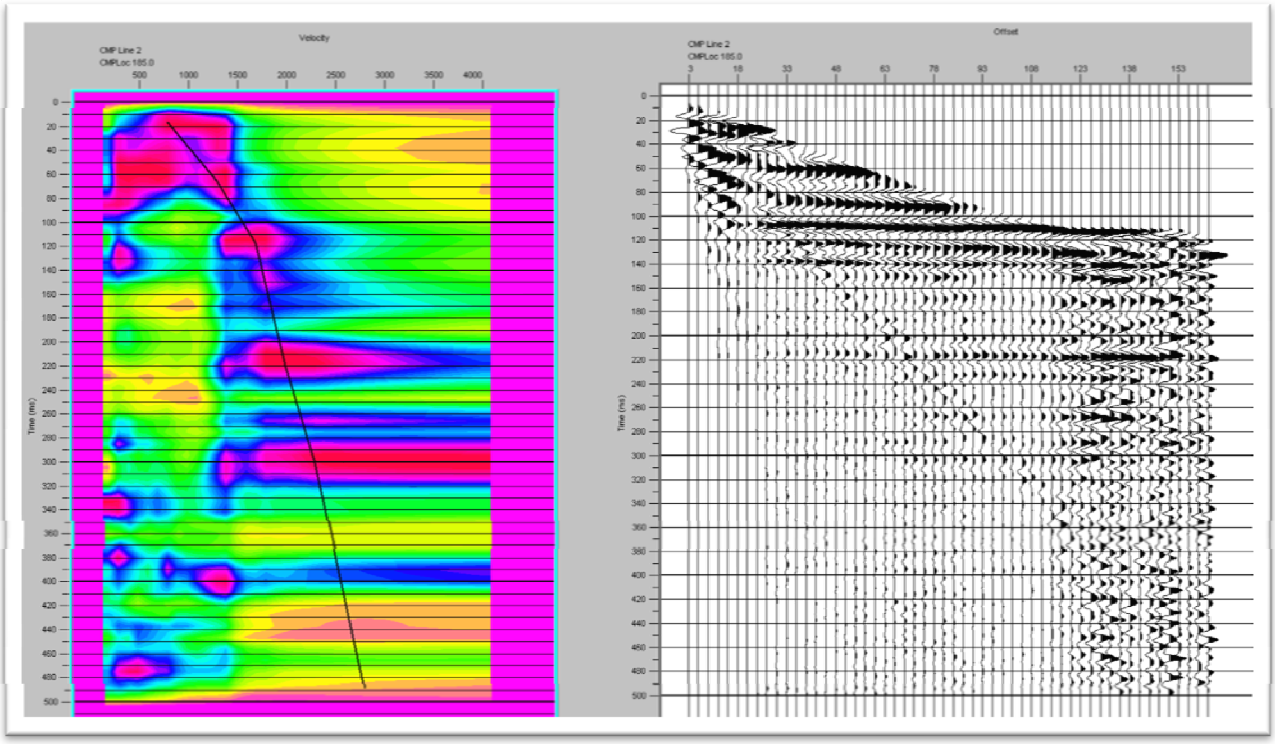

Figure 6. Example of CMP supergather velocity analysis from Line MA09-01. The colored figure on the left shows semblance as a function of velocity (horizontal axis) and time (vertical axis). The figure on the right is a CMP supergather that has been corrected for NMO using the velocity function that has been interactively picked (black line) on the left-hand figure. The circular bullseye in the semblance plot at 100-130 ms indicates a well-constrained velocity that is defined by a coherent reflector over an adequate offset range.

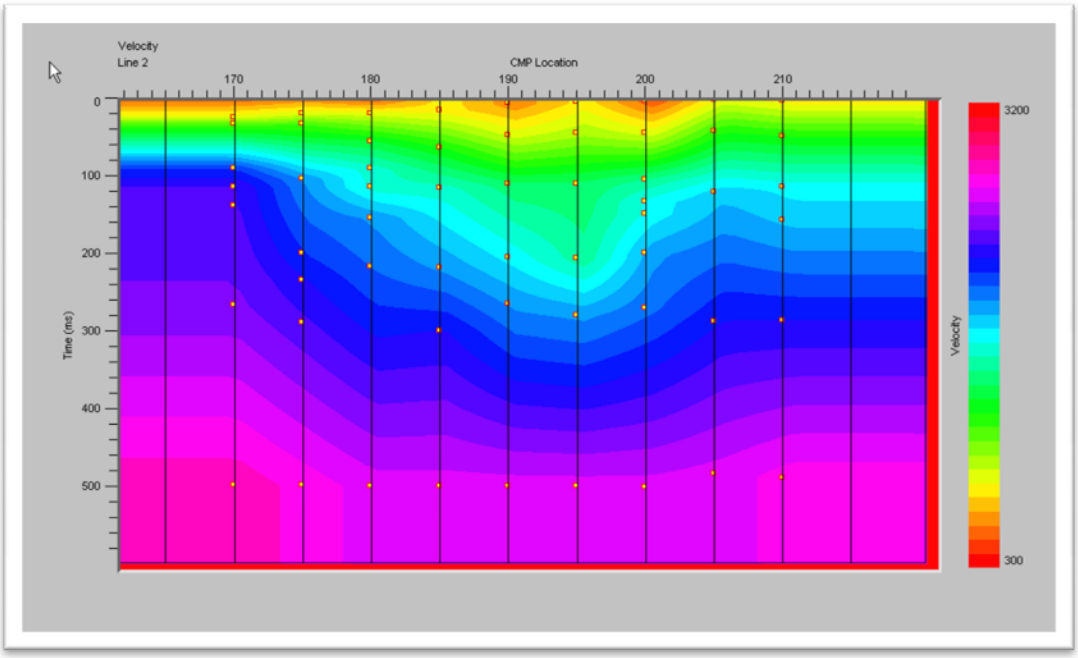

Figure 7. Velocity field for line MA09-02. Each of the vertical black lines indicates the location of a CMP supergather and semblance velocity analysis, as shown in Figure 6 above. The point symbols indicate velocity picks.

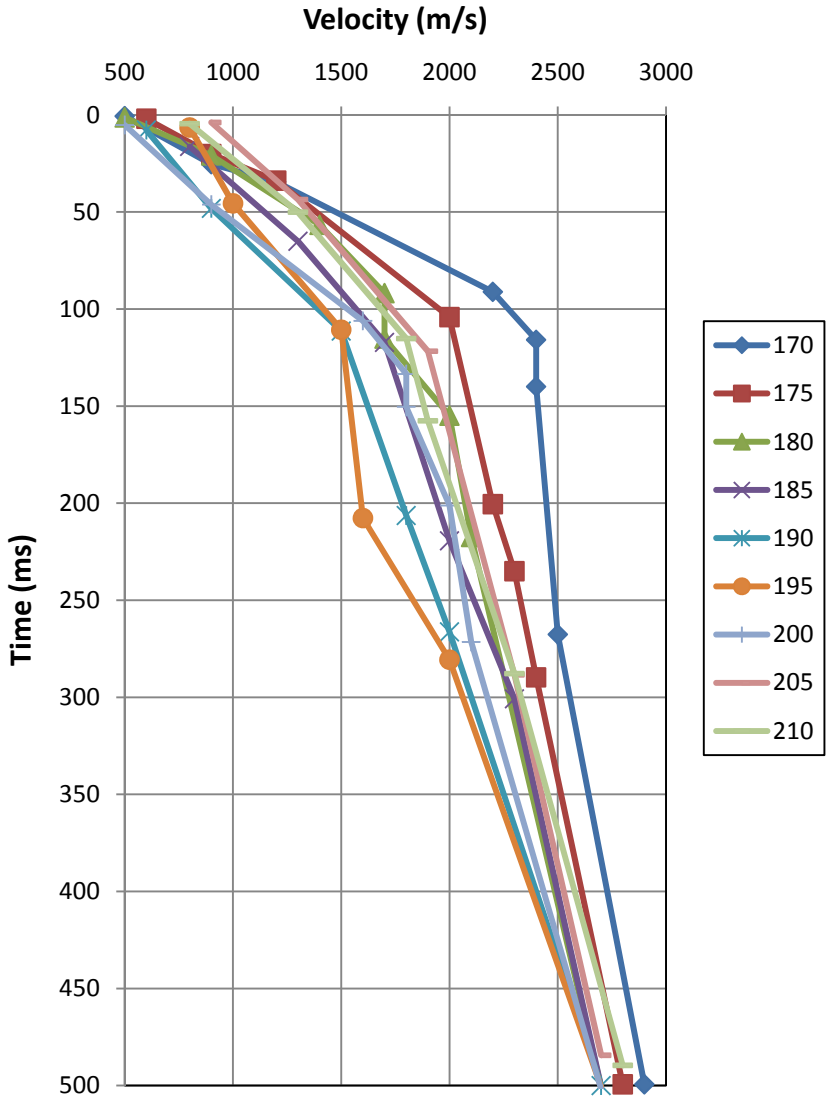

Figure 8. Stacking velocities from Line MA09-02. Each line is a velocity function from a different velocity analysis location. Symbols are picks from semblance velocity analysis and correspond to the velocities shown in Figure 7 above.

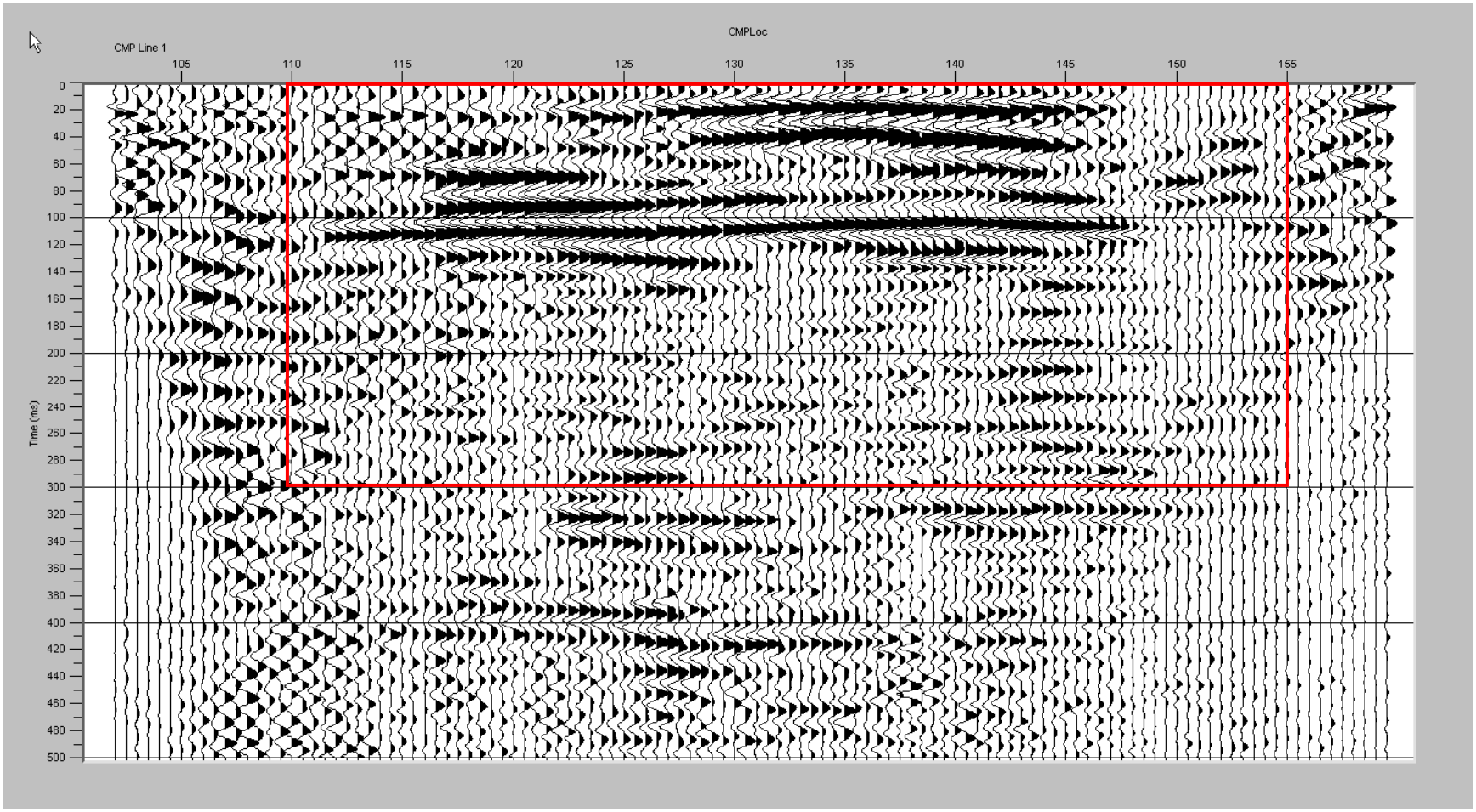

Figure 9. Seismic reflection profile MA09-01. The red box indicates the extent of the data shown in Figure 12a.

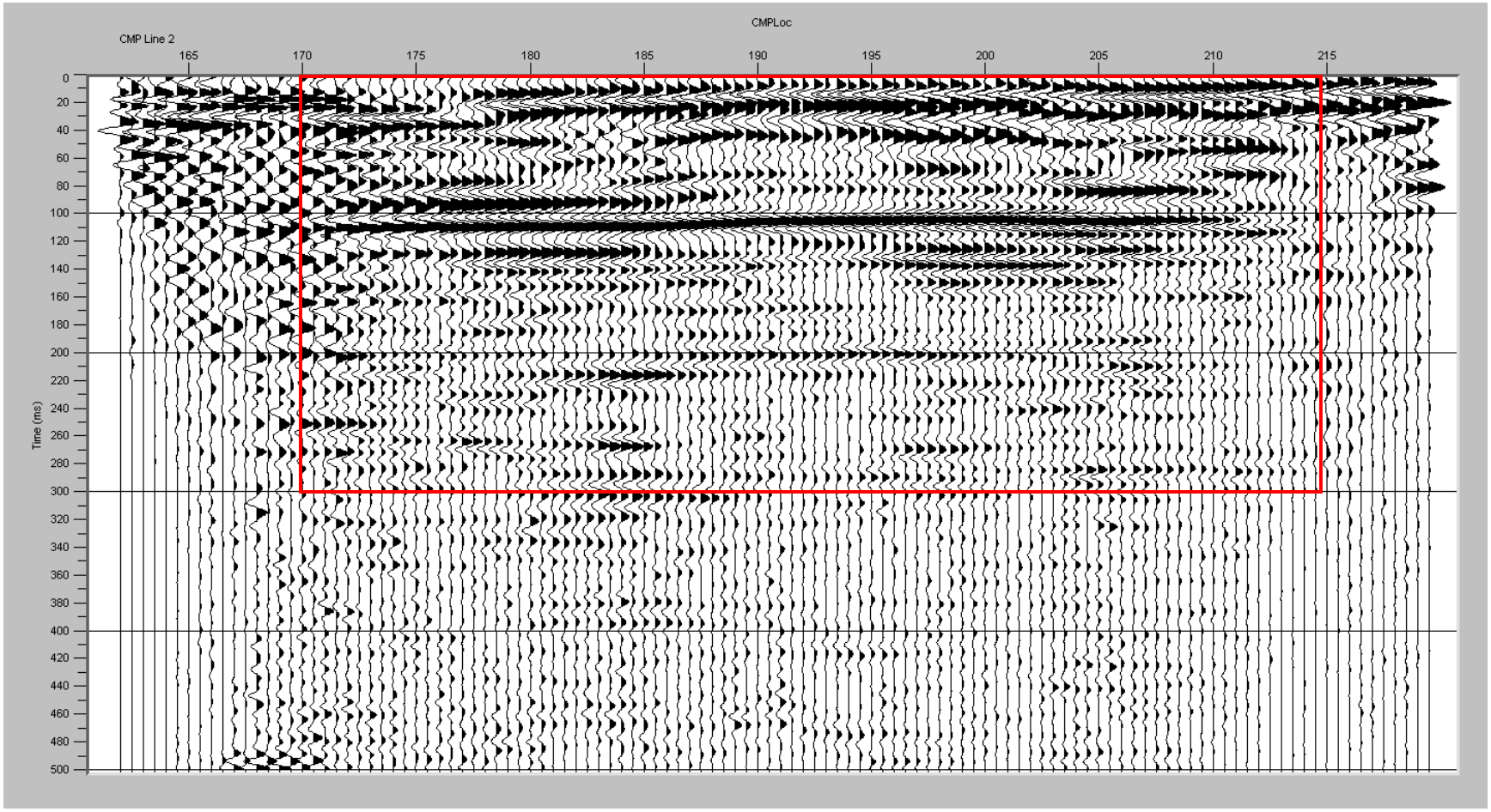

Figure 10. Seismic reflection profile MA09-02. The red box indicates the extent of the data shown in Figure 12b.

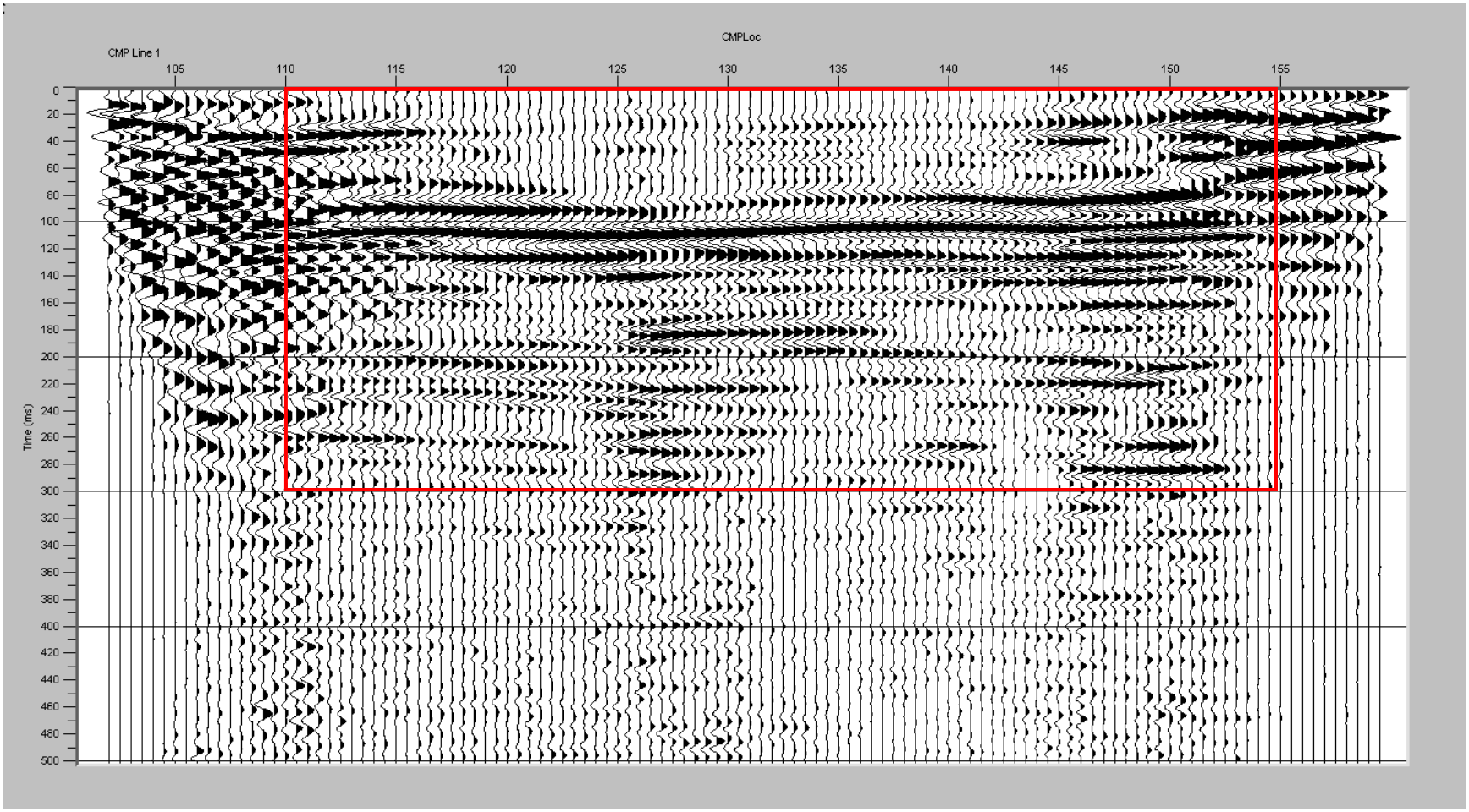

Figure 11. Seismic reflection profile MA09-03. The red box indicates the extent of the data shown in Figure 12c.

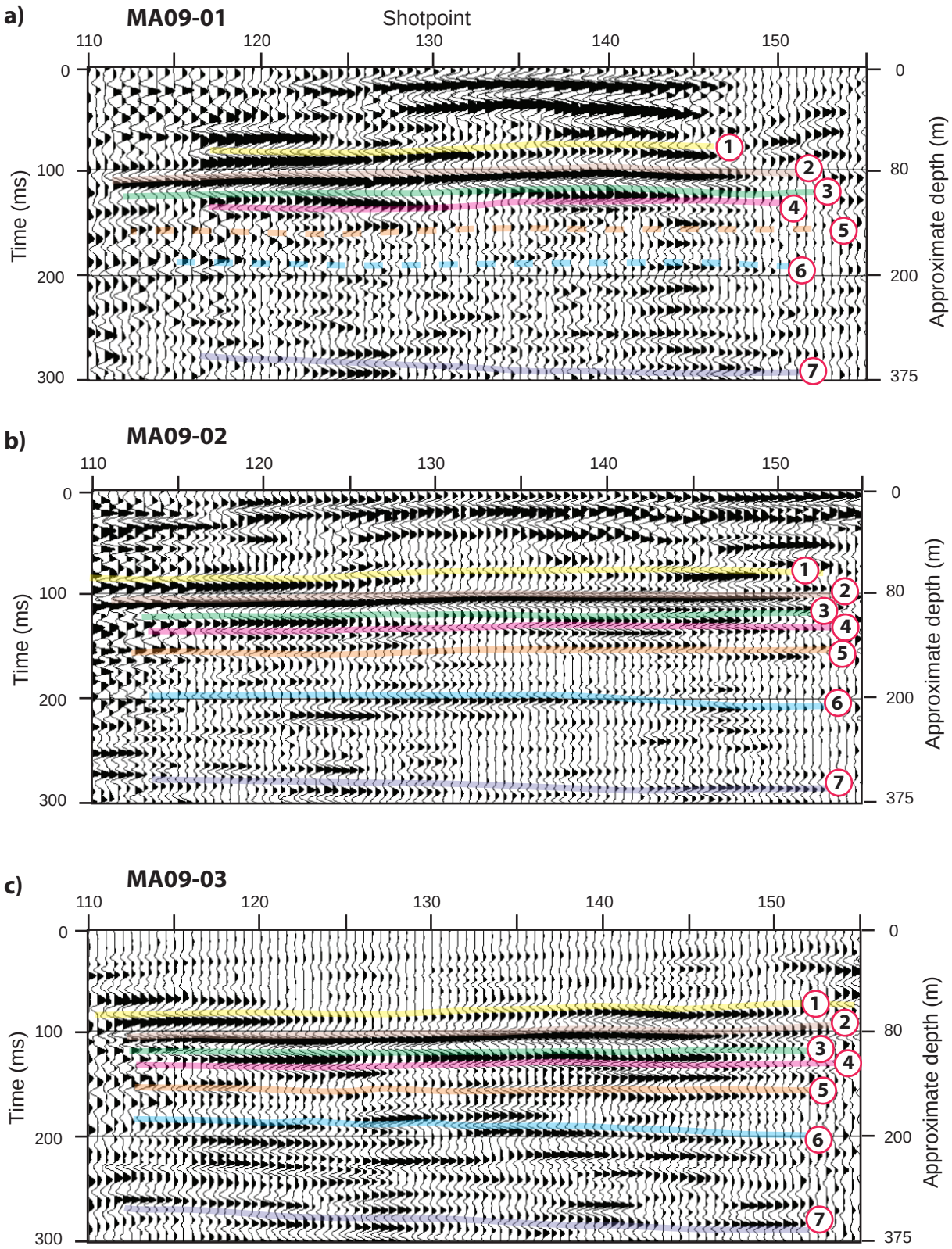

Figure 12. Seismic profiles and interpretations for a portion of seismic lines a) MA09-01, b) MA09-02, and c) MA09-03. Selected horizons common to all three lines are indicated in color and labeled 1-7. Times are two-way travel times. Labeled depths are estimated based on stacking velocities from Line MA09-02. Sections are unmigrated. The complete uninterpreted profiles are shown in Figures 9-11.